

The SOL turbulence characteristics in the first experimental campaign on W7-X

S. C. Liu^{1,2}, Y. Liang¹, P. Drews¹, D. Nicolai¹, G. Satheeswaran¹, K. P. Hollfeld¹, N. Sandri¹, D. Höschen¹, N. C. Wang¹, A. Krämer-Flecken¹, M. Henkel¹, M. Rack¹, X. Han¹, E. H. Wang¹, Y. L. Wei¹, J. Q. Cai¹, Y. Gao¹, O. Neubauer¹, O. Grulke³, R. König³, J. Geiger³ and W7-X Team

¹ Forschungszentrum Jülich GmbH, Institut für Energie- und Klimaforschung – Plasmaphysik, Partner of the Trilateral Euregio Cluster (TEC), 52425 Jülich, Germany

² Institute of Plasma Physics, Chinese Academy of Sciences, Hefei 230031, People's Republic of China

³ Max-Planck-Institute for Plasma Physics, 17491 Greifswald, Germany

Email: sh.liu@fz-juelich.de

Abstract

Turbulence is considered to play an important role in the edge cross field heat and particle transport in fusion devices. The SOL turbulence characteristics were measured by the combined probe mounted on the fast manipulator during the first experimental campaign of W7-X. The combined probe head, consisting of triple probe, Mach probe and two sets of 3D magnetic coils, are capable to measure edge profiles of T_e , n_e , floating potential, parallel Mach number, local magnetic field, electrostatic and electromagnetic fluctuations. With this setup of probe head, the turbulence correlation length, decorrelation time, propagation behaviour along both radial and poloidal directions can be obtained. The poloidal cross correlation spectrum $S(k_\theta, f)$, representing the dispersion relation in k_θ and f space, shows that the dominant fluctuations have a frequency below 60 kHz, and their phase velocity and group velocity shift to the direction of ion diamagnetic drift with decreasing the distance to the last closed flux surface ($R-R_{LCFS}$) in the limiter plasma on W7-X. Both the poloidal and radial correlation lengths are in the range of 5-10 mm. A low frequency mode around 7 kHz has been observed by both Langmuir probes and magnetic probes, and it can propagate to the far SOL (about $R=6.15$ m). The amplitude of this mode has strong dependence on magnetic topology.

1. Introduction

Turbulence is considered to play an important role in the edge cross field heat and particle transport in magnetized plasmas of fusion devices, because the transport is generated dominantly by plasma fluctuations. For example, the intensive heat and particle exhaust during the eruption of edge localized mode (ELM) in tokamak is driven by peeling-ballooning modes which link to pressure gradient and current gradient [1]. An electrostatic coherent mode produces significant outflow of particles and heat and in consequence greatly facilitating the long H-mode sustainment in EAST tokamak [2]. In stellarator, edge turbulence behaviours largely depend on the 3D magnetic topology, especially

magnetic islands and stochastization of magnetic field. Plenty of 3D physics issues have been studied in large helical device (LHD), such as the transport, bifurcation physics, flow damping and shear [3, 4].

Wendelstein 7-X (W7-X), a stellarator with inherent 3D magnetic topology, has large stochastic field region and islands on plasma edge. During the first experiment (OP1.1) on W7-X, the scrape-off layer (SOL) plasma profiles and turbulence behaviors are measured by a combined probe mounted on fast manipulator. In this paper, the SOL turbulence characteristics will be presented as following: experimental setup, experimental results, discussion and conclusion.

2. Experimental setup

W7-X is a new generation of optimized stellarator with superconducting coil system to accommodate a variety of 3D magnetic configurations, aiming to achieve quasi-steady state operation with plasma parameters close to the future fusion power plant. Its major radius is 5.5 m [5]. In order to study edge plasma properties, a combined probe head consisting of Langmuir probes, Mach probe and two three-dimension magnetic coils was mounted on the fast manipulator in OP1.1 of W7-X, is able to measure electron density n_e , temperature T_e , floating potential, radial electric field and parallel flow velocity, the variation of magnetic fields in directions of (R, φ, Z) and turbulence structures [6-8]. The multi-purpose manipulator is located at the outer midplane of module four at AEK40 flange with a maximum fast plunge length of 35 cm and maximum speed of 2 m/s.

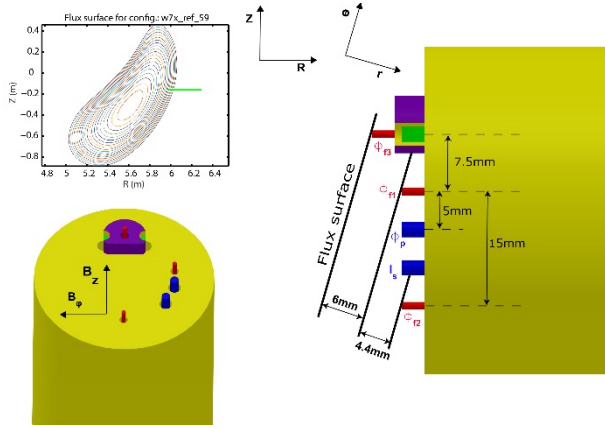


Figure 1. The sketch of combined probe head in OP1.1 on W7-X. The magnetic equilibrium shown in left top is standard limiter configuration, with probe path labelled in green line.

As shown in Figure 1, Pins ' ϕ_{f1} ', ' ϕ_{f2} ' and ' ϕ_{f3} ' with 1 mm diameter measure floating potential, while ' ϕ_p ' and ' I_s ' with 2 mm diameter consist of a double probe. There is an angle of $\sim 17^\circ$ between the probe plane and the local flux surface in OP1.1, which make it impossible to extract the poloidal information of turbulence from pins ' ϕ_{f1} ' and ' ϕ_{f2} ' because they are located in two absolutely different flux surfaces. However, when ' ϕ_p ' measures floating potential by switching off the biasing voltage between ' ϕ_p ' and ' I_s ' the turbulence poloidal structure can be obtained from ' ϕ_{f1} ' and ' ϕ_p '. The radial correlation is derived from ' ϕ_{f1} ' and ' ϕ_{f3} ' separated by 6.7 mm radially. The temporal resolution of fast probe is 1 MHz.

3. Results and discussion

3.1. Fluctuations power spectrum

The fluctuations of floating potential and ion saturation current for a typical discharge in OP1.1 are shown in Figure 2, with electron cyclotron resonance heating (ECRH) power of 3.2 MW, line averaged density about $1.5 \times 10^{19} \text{ m}^{-3}$, standard limiter configuration. The fluctuations are relatively low in far SOL due to block effects of first wall components, while increase sharply to huge amplitudes when $R < 6.08 \text{ m}$ with last closed flux surface (LCFS) located at $R = 6.03 \text{ m}$. Noted here the relative fluctuation level of ion saturation current is much higher than floating potential, indicating strong fluctuating particle flux in near SOL. The negative spike of ion saturation may come from fast electrons which is probably due to the injection of ECRH.

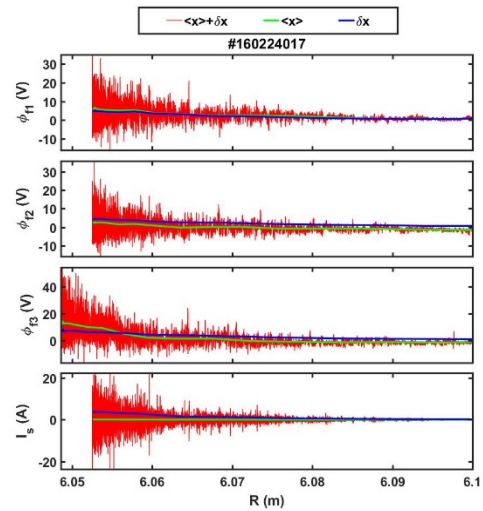


Figure 2. Fluctuation level of floating potential and ion saturation current.

Figure 3 shows the plasma parameter of the experimental shots on day 160223 and shot #160224028, with ECRH power 2 MW and 3.2 MW, separately. The auto correlation power spectrums of floating potential and toroidal magnetic field are shown in Figure 4. $P_{xx}^j(f) = X^j(f)X^{j*}(f)$, where $X^j(f)$ is the Fourier transform of signal $x(t)$, and the star signifies complex conjugate. There is a broad spectrum in floating potential and its power density increases with decreasing $R - R_{LCFS}$. The magnetic coil signal also exhibits similar increases of auto correlation power when near separatrix. Both

Langmuir probe and magnetic coil observe an electromagnetic coherent mode (EMCM) with frequency near 7 kHz, which starts to appear when $R < 6.15$ m in standard limiter configuration for Langmuir probes but can be seen inside vessel port for magnetic coils. In addition a broad spectrum with central frequency at 115 kHz appears only on magnetic coil signals.

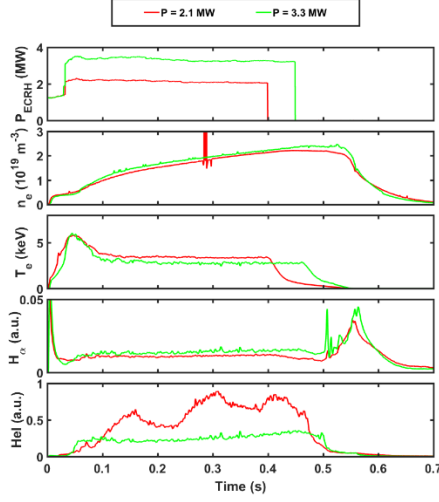


Figure 3. Plasma parameters for the experimental shots on day 160223 and shot #160224028.

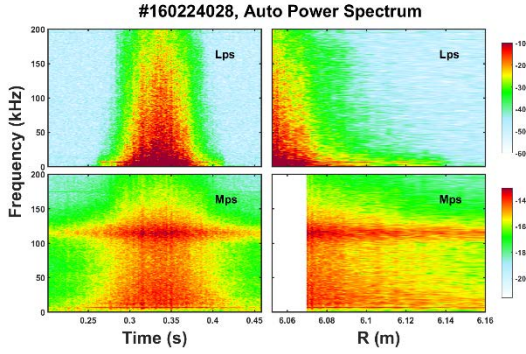


Figure 4. Spectrogram of floating potential and toroidal magnetic field measured by reciprocating probe.

3.2. Turbulence power spectrum and propagation

For these shots, the biasing voltage of the triple probe is switched off, in consequence the pin ' ϕ_p ' measuring floating potential can be used to calculate poloidal correlations. The wavenumber-frequency spectral density $S(k, f)$ can be derived from the two-point correlation techniques [9]. The poloidal correlation spectral $S(k_\theta, f)$ is illustrated in Figure 5 for 9 radial

positions. The cross correlation power increases clearly from $R = 6.15$ m, and most power is distributed in low frequency range (< 60 kHz). In the range of $R = 6.09$ - 6.15 m poloidal correlation spectral reveals symmetric distribution along k_θ space, while favors ion diamagnetic drift (ω_{*i}) gradually with decreasing R - R_{LCFS} . When probe is close to LCFS the group velocity of turbulence is in ω_{*i} direction, with speed about 0.1 km/s. Noted the EMCM is highlighted in the range of $R = 6.09$ to 6.13 m, tending to propagate in electron diamagnetic drift direction (ω_{*e}).

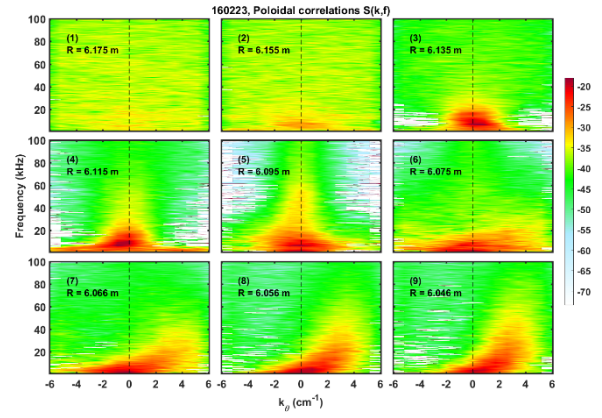


Figure 5. The normalized poloidal correlation spectral $S(k_\theta, f)$ in a radial position scan experiment. Positive k_θ denotes the direction of ion diamagnetic drift.

The statistical properties of turbulence within frequency range of 1-200 kHz are shown in Figure 6. Usually a normalized dispersion relationship 'conditional spectrum' $S(k|f) = S(k, f)/S(f)$ is also used to illustrate the turbulence characteristics. The turbulence mean phase velocity is calculated by $V_{ph} = \sum_{k,f} 2\pi f S(k, f)/k$ [10, 11]. In laboratory frame, the turbulence phase velocity V_{ph} is given by the $E \times B$ drift velocity plus plasma-frame phase velocity V_{plasma} . In low heating edge plasma, if $V_{E \times B} \gg V_{plasma}$, we have $E_r \cong V_{ph} B$ [12]. In our experiment, the radial electric field derived from $E_r = -d(\phi_f + 2.8T_e)/dr$ has similar curve with that from turbulence phase velocity but higher amplitude. Fluctuations correlation length is defined as $l_c = 1/\langle \sigma_k \rangle$, where

$$\langle \sigma_k^2 \rangle = \sum_f \{ \sum_k [k - \bar{k}(f)]^2 S(k|f) \} S(f) \quad \text{and} \quad \bar{k}(f) = \sum_k k \cdot S(k|f).$$

The poloidal correlation length is

about 0.5-0.8 cm and tends to increase in near SOL. The two poloidal separated floating potential pins have high correlation coefficient, and also increase in near SOL. Both poloidal and radial averaged frequency decreases to 15-20 kHz when $R < 6.14$ m, indicating low frequency dominated turbulence in most SOL. Compared to poloidal correlation, radial phase velocity is smaller and almost zero in near SOL; the correlation length is about 0.4 cm in near SOL. It is obvious that in the region of $R = 6.09 - 6.13$ m both connection length and correlation coefficient have peak values. In contrast, the poloidal phase velocity reaches its minimum at the same position. As shown in Figure 5, relatively high cross correlation power near 7 kHz is displayed in this radial region. As mentioned before, the turbulence group velocity in near SOL is toward ω_{*i} direction but EMC has tends to propagate in ω_{*e} direction, which is consistent with the decrease of poloidal phase velocity in this high correlation region. The EMC has very strong dependence on radial location, which probably relates to magnetic topology. On the other hand, the shot #160224028 with higher heating power has negative minimum poloidal phase velocity but higher correlation coefficient, because there is an ECRH power threshold for EMC and the mode is enhanced in high P_{ECRH} case.

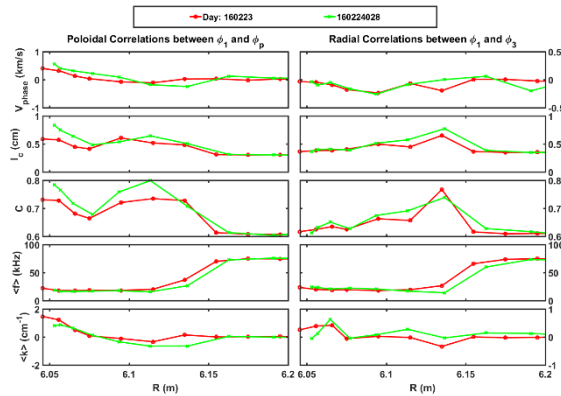


Figure 6. Statistical properties of turbulence, they are turbulence phase velocity V_{phase} , connection length, correlation coefficient, averaged frequency and averaged wave number from top to bottom. The left panels are poloidal correlation while right panels are radial correlation. Noted the positive poloidal phase velocity denotes ion diamagnetic drift direction, and positive radial phase velocity is outward.

4. Conclusion

The SOL electrostatic and magnetic fluctuations are measured by reciprocating probes in the first experimental campaign on W7-X. Low frequency turbulence is dominant in SOL. The poloidal correlation length of turbulence is about 0.5-0.8 cm, while radial correlation length is a little smaller. In near SOL the averaged frequency decreases to about 15-20 kHz, and the turbulence mean phase velocity is comparable to $E \times B$ drift velocity. An EMC can be seen by Langmuir probes within $R = 6.15$ m in standard limiter configuration, and exhibits strong dependence on magnetic topology. EMC has an ECRH power threshold that may vary according to plasma condition. In future, more dedicated work will be continued to give a physical image of EMC in SOL.

Acknowledgement

This work has been carried out within the framework of the EUROfusion Consortium, has received funding from the Euratom research and training programme 2014-2018 under grant agreement No 633053, and was supported by the National Natural Science Foundation of China under Grant Nos. 11405213. The views and opinions expressed herein do not necessarily reflect those of the European Commission.

Reference

- [1] P. B. Snyder *et al.* 2005 Phys. Plasmas 12 056115
- [2] H. Q. Wang *et al.* 2014 Phys. Rev. Lett. 112 185004
- [3] K. Ida *et al.* 2015 Nat Commun 6 5816
- [4] K. Ida *et al.* 2016 Nucl. Fusion 56
- [5] T. S. Pedersen *et al.* 2016 Nat Commun 7 13493
- [6] Y. Liang *et al.* 2017 Nucl. Fusion 57 066049
- [7] D. Nicolai *et al.* 2017 Fusion Eng. Des.
- [8] P. Drews *et al.* 2017 Nucl. Fusion 57 Submitted
- [9] J. M. Beall *et al.* 1982 J. Appl. Phys. 53 3933
- [10] T. Uckan *et al.* 1990 J. Nucl. Mater. 176 693
- [11] Y. Xu *et al.* 2007 Nucl. Fusion 47 1696
- [12] J. H. Yu *et al.* 2007 J. Nucl. Mater. 363 728